

Microfluidic Circuit Dynamics and Control for Caterpillar-Inspired Locomotion in a Soft Robot

Helene Nguewou-Hyousse¹, Giulia Franchi², and Derek A. Paley³

Abstract—Because caterpillars can locomote through complex terrain, caterpillar-inspired soft robots promise safe and reliable access for search, rescue, and exploration. Microfluidic components analogous to electronic components like resistors and capacitors further promise the principled design and fabrication of autonomous soft robots powered by microfluidic circuits. This paper presents a model for caterpillar locomotion using an oscillator network approach, in which the periodic motion of each leg is described by an oscillator, and the collection of all legs forms a network. We use tools from graph theory to model (1) a first-order system consisting of a network of RC oscillators connected to an astable multivibrator circuit serving as a Central Pattern Generator (CPG); and (2) a second-order system consisting of a network of RLC oscillators with a deCentralized Pattern Generator (dCPG) as reference control. For the RC network, we analyze the rate of convergence and the gait number, a metric that characterizes the locomotion gait. For the RLC network, we design feedback laws to stabilize consensus and traveling wave solutions. Numerical modeling and preliminary experimental results show promise for the design and control of locomotion circuitry in a caterpillar-inspired soft robot.

I. INTRODUCTION

Robots made from soft materials are more flexible and may be more capable of adapting to complex environments than rigid robots. As such, their applications range from search and rescue to exploration and medicine [1], [2]. Soft robots inspired by organisms without a skeleton may also be easier to design and fabricate than vertebrate-inspired robots, because of the level of abstraction offered by the simplicity of their anatomy [3]. A caterpillar is an example of a soft-bodied animal that can navigate irregular and vertical terrains [4]. Caterpillar locomotion exhibits (i) the synchronous motion of left-right pairs of legs, and (ii) a wave propagation pattern traveling from tail to head [4]–[6]. Thus, a caterpillar-inspired soft-robotic system should be capable of collective behavior such as synchronization and wave propagation. Furthermore, choosing appropriate fabrication material [3] and structure geometry should guarantee its flexibility.

The motivation behind this work is the design and closed-loop control of a novel locomotion mechanism in a caterpillar-inspired soft robot. We seek to design a 3D-printed caterpillar robot with internal microfluidic circuitry that drives leg actuation. When an actual caterpillar moves, each left-right pair of legs is lifted simultaneously and goes through a stance phase and a swing phase [5], [6]. In addition, a wave is repeatedly generated at the terminal proleg and travels to the front leg, creating a periodic behavior that can be modeled by an oscillator network with a cyclic topology.

Electrical circuits may be used to represent microfluidic circuits using Equivalent Circuit (EC) Theory [7]. Although not all electrical components have a microfluidic analog (e.g., there are no microfluidic inductors due to low inertial effects at the millimeter scale), EC supports the design of microfluidic circuits and robots. For example, the Octobot is an octopus-inspired autonomous soft robot with microfluidic logic fabricated using soft lithography [1]. However, recent trends in microfluidics have demonstrated the viability of 3D-printed circuit components [8]; using this technique to print a microfluidic soft robot would reduce the need for circuit interconnections and may simplify design and fabrication. An astable multivibrator [1], [9], for example, is an oscillating circuit that can be implemented with either electric or microfluidic components.

This paper considers a coordinated network of fluidic oscillators generating and controlling periodic leg actuation. Previous work on modeling caterpillar-inspired locomotion in a soft body applied inverse-dynamics to a planar extensible-link model [10], or lumped-mass dynamic model coupled with a control law for gait optimization [2], [4]. Autonomous decentralized control is a solution to generating and controlling local and adaptive locomotion in soft robots [11], [12]. In particular, Umedachi and Trimmer implemented an autonomous decentralized control to extend and contract segments of a 3D printed modular soft robot; the results show that implementing modular deformity resulted in a phase gradient that induced locomotion [11].

Prior work in the area of collective motion of networked oscillators used a spatial approach to look at the phases of each oscillator [13], [14]. Here we investigate feedback control of an oscillator network to generate cyclic actuation of many individual legs. We study both first- and second-order dynamical models. For the first-order model, which consists of a multivibrator circuit driving a set of RC oscillators in series, we introduce a gait number to characterize the locomotion pattern. For the second-order model, which

*This work is supported by ARO Grant No. W911NF1610244

¹Helene Nguewou-Hyousse is a graduate student in the Department of Electrical and Computer Engineering, University of Maryland, College Park, MD 20742, USA hnguewou@umd.edu

²Giulia Franchi is Assistant Professor of Computer Science in the Department of Mathematics and Computer Science, Salisbury University, Salisbury, MD 21801, USA gxfranchi@salisbury.edu

³Derek A. Paley is the Willis H. Young Jr. Professor of Aerospace Engineering Education in the Department of Aerospace Engineering and the Institute for Systems Research, University of Maryland, College Park, MD 20742, USA dpaley@umd.edu

consists of a network of RLC circuits in a cyclic topology, we modify the network to include a deCentralized Pattern Generator (dCPG) as the decentralized control. For example, in consensus control of multiple oscillators, the dCPG sets the collective phase, but the phase lags if the network itself is lagging.

The contributions of this paper are (1) the design of a first-order RC oscillator network model for generating caterpillar-inspired locomotion in a microfluidic circuit, and the characterization of the resulting locomotion gait; (2) the design of a second-order RLC oscillator network model, and closed-loop feedback control laws for consensus and traveling wave solutions; and (3) the inclusion of a deCentralized Pattern Generator to regulate the collective phase of the consensus solution in the RLC network. This work demonstrates cooperative behavior of a network of oscillator circuits compatible with microfluidics; it also proposes a model for the closed-loop control design of an RLC network to produce stable cyclic motion. These steps provide a theoretical approach to the study of legged locomotion in an autonomous soft robot using microfluidics; we also include preliminary results from our ongoing experimental testbed.

The paper is organized as follows. Section II presents an overview of RLC oscillators, algebraic graph theory, first- and second-order consensus dynamics, and microfluidic circuit theory. Section III-A provides a mathematical framework for the RC network model and presents an analysis of its convergence properties, including a parametrization of the locomotion gait. Section III-B contains a mathematical framework for the RLC network, including open-loop stability analysis, closed-loop control design for consensus and traveling wave solutions, and the effect of the dCPG. Section IV presents preliminary experimental results from ongoing work with the RC microfluidic network. Section V summarizes the paper and our future work.

II. BACKGROUND

The proposed work models each leg of a caterpillar as an RLC (or RC) circuit. The network of N caterpillar legs is connected in either a circulant or a chain topology. In the microfluidic testbed, pressure is analogous to voltage, whereas volumetric flow rate is analogous to current. In a pneumatic setting, each microfluidic leg will be actuated by internal pressure; we use Equivalent Circuit theory to design these pressure inputs using electrical circuits. This section first reviews RLC and RC circuits, followed by a background overview of graph theory, consensus dynamics, and the field of microfluidics.

A. RLC and RC Circuit Theory

Kirchoff's loop equation for a series RLC circuit with resistance r , inductance l , capacitance c , current i , and input voltage $V(t)$ is $v_r + v_c + v_l = V(t)$, where $v_l = l di/dt$, $v_r = ri$ and $v_c = \frac{1}{c} \int_{-\infty}^t i(\tau) d(\tau)$ [15]. Defining state variables $v = v_c$ and $a = \dot{v}_c$, the system dynamics have

the following linear state-space representation:

$$\frac{d}{dt} \begin{bmatrix} v \\ a \end{bmatrix} = \begin{bmatrix} 0 & 1 \\ -\frac{1}{lc} & -\frac{r}{l} \end{bmatrix} \begin{bmatrix} v \\ a \end{bmatrix} + \begin{bmatrix} 0 \\ \frac{1}{lc} \end{bmatrix} V(t).$$

The circuit oscillates if it is underdamped, i.e., when $r^2 c < 4l$. In the absence of an inductor, i.e., in a microfluidic circuit, we have a resistor-capacitor (RC) circuit in series, which is governed by the first-order equation

$$c\dot{v} + \frac{v}{r} = \frac{1}{r} V(t).$$

The time constant of $\tau_1 = rc$ represents the time required for the voltage at the capacitor to drop to $v(0)/e$.

B. Algebraic Graph Theory

Graph theory is used to represent the topology of the oscillator network in which each leg is represented as a node. The Laplacian matrix \mathcal{L} defines the connections between the nodes of the network. Given the undirected graph $\mathcal{G} = (\mathcal{V}, \mathcal{E})$ with vertex set \mathcal{V} of cardinality N and edge set \mathcal{E} , we write the Laplacian matrix as $\mathcal{L} = D - A$. The adjacency matrix $A \in \mathbb{R}^{N \times N}$ is symmetric, with entries $a_{ij} = a_{ji}$ given by

$$a_{ij} = \begin{cases} 1, & \text{if } i \neq j \text{ and } (i, j) \in \mathcal{E} \\ 0, & \text{otherwise.} \end{cases}$$

The degree matrix $D \in \mathbb{R}^{N \times N}$ has the ij^{th} entry

$$d_{ij} = \begin{cases} \sum_{j=1}^N a_{ij}, & \text{if } i = j \\ 0, & \text{otherwise.} \end{cases}$$

The Laplacian of an undirected graph is a symmetric, positive semi-definite matrix with zero row sums. For example, the Laplacian matrix of an undirected chain graph with N edges is

$$\mathcal{L}_1 = \begin{bmatrix} 1 & -1 & 0 & \cdots & 0 \\ -1 & 2 & -1 & 0 & \cdots & 0 \\ 0 & -1 & 2 & -1 & 0 & \cdots & 0 \\ \vdots & \ddots & \ddots & \ddots & \ddots & & \vdots \\ \vdots & & \ddots & \ddots & \ddots & \ddots & \\ \vdots & & & \ddots & -1 & 2 & -1 \\ 0 & 0 & \cdots & 0 & -1 & 2 & 1 \end{bmatrix} \in \mathbb{R}^{N \times N}, \quad (1)$$

whereas the Laplacian matrix of an undirected cyclic graph with degree 2 is

$$\mathcal{L}_2 = \begin{bmatrix} 2 & -1 & 0 & \cdots & -1 \\ -1 & 2 & -1 & 0 & \cdots & 0 \\ 0 & -1 & 2 & -1 & 0 & \cdots & 0 \\ \vdots & \ddots & \ddots & \ddots & \ddots & & \vdots \\ \vdots & & \ddots & \ddots & \ddots & \ddots & \\ \vdots & & & \ddots & -1 & 2 & -1 \\ -1 & 0 & \cdots & 0 & -1 & 2 & 2 \end{bmatrix} \in \mathbb{R}^{N \times N}. \quad (2)$$

Note that \mathcal{L}_2 is a circulant matrix, i.e, each row vector is a cyclic permutation of the preceding row vector.

C. Consensus Theory

Depending on the network topology, it is often possible to achieve collective behavior via consensus. Consensus refers to a group of agents achieving a common decision or behavior over time through a local distributed protocol [16]–[18]. Consider the linear consensus scheme [19]

$$\dot{\mathbf{v}} = -\mathcal{L}\mathbf{v},$$

where $\mathbf{v} = [v_1, \dots, v_N]^T \in \mathbb{R}^N$ and \mathcal{L} is a graph Laplacian. Previous work [19], [20] showed that this system eventually achieves first-order consensus, i.e., $v_j = v_k$ for all pairs j and k , if the associated communication graph \mathcal{G} has a spanning tree. \mathcal{G} has a directed spanning tree if and only if \mathcal{L} has a simple zero eigenvalue (with associated eigenvector $\mathbf{1}_N$) and all other eigenvalues have positive real parts. Furthermore, $e^{-\mathcal{L}t} \rightarrow \mathbf{1}_N \mathbf{p}^T$ and $v_i(t) \rightarrow \sum_{i=1}^N (p_i v_i(0))$ as $t \rightarrow \infty$, where $\mathbf{p} = [p_1, \dots, p_N]^T \geq 0$ is a left eigenvector of \mathcal{L} associated with the simple zero eigenvalue and $\sum_{i=1}^N p_i = 1$.

Consider N coupled harmonic oscillators with local interaction of the form [16]

$$\frac{d}{dt} \begin{bmatrix} \mathbf{v} \\ \mathbf{a} \end{bmatrix} = \begin{bmatrix} \mathbf{0}_N & \mathbf{I}_N \\ -\alpha \mathbf{I}_N & -\mathcal{L} \end{bmatrix} \begin{bmatrix} \mathbf{v} \\ \mathbf{a} \end{bmatrix},$$

where $\mathbf{0}$ denotes the $N \times N$ zero matrix, \mathbf{I} denotes the $N \times N$ identity matrix, and \mathcal{L} is a Laplacian matrix associated with directed graph \mathcal{G} . There exists right eigenvector $\mathbf{1}_N$ satisfying $\mathcal{L}\mathbf{1}_N = 0$ and left eigenvector $\mathbf{p} \in \mathbb{R}^N$ satisfying $\mathbf{p} \geq 0$, $\mathbf{p}^T \mathcal{L} = 0$, and $\mathbf{p}^T \mathbf{1}_N = 1$. The N agents achieve second-order synchronization if \mathcal{G} has a directed spanning tree [16]. More specifically, $v_i(t) \rightarrow \cos(\sqrt{\alpha t}) \mathbf{p}^T \mathbf{v}(0) + (1/\sqrt{\alpha}) \sin(\sqrt{\alpha t}) \mathbf{p}^T \mathbf{a}(0)$ and $a_i(t) \rightarrow -\sqrt{\alpha} \sin(\sqrt{\alpha t}) \mathbf{p}^T \mathbf{v}(0) + \cos(\sqrt{\alpha t}) \mathbf{p}^T \mathbf{a}(0)$ as $t \rightarrow \infty$.

D. Microfluidic Circuit Theory

Microfluidics refers to the precise manipulation of fluidic networks at the submillimeter level [21], [22]. Microfluidic components include diodes, capacitors, transistors, and hydraulic resistances. Microfluidic circuits can be analyzed using computational fluid dynamics (CFD) analysis, although as the number of circuit components to be modeled increases, the CFD analysis becomes complex. Electric circuit theory is an alternative technique that uses the analogy between fluidic and electronic components to describe the dynamics of a microfluidic circuit using electrical equations [22], [7]. Pressure, volumetric flow rate, and hydraulic resistance are equivalent to voltage, current, and electric resistance, respectively. By making the assumption that the fluidic flow is laminar, viscous, and incompressible, the use of electric circuit theory greatly simplifies the analysis of the flow dynamics in microfluidic circuits. Microfluidic circuit theory applied to robotics is relevant because it promises to enable the design and fabrication of autonomous microfluidic soft robots; moreover, using 3D-printing techniques to fabricate the microfluidic components and integrate with a soft body may allow the fabrication of an autonomous fully integrated soft robot [21].

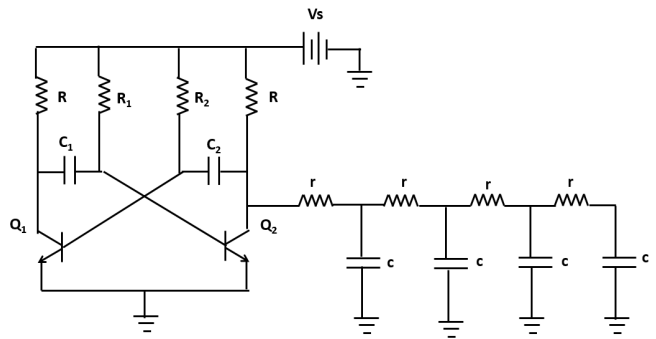


Fig. 1: Schematic of an astable multivibrator connected to an RC network with $N = 4$

III. DYNAMICAL MODELS

This section contains the mathematical framework governing the dynamics of two oscillator networks. Section III-A describes an RC network driven by a multivibrator oscillator, and Section III-B describes an RLC network with control inputs at each node. The RLC network incorporates a dCPG as reference input to regulate the collective phase.

A. First-Order System: RC Network

Motivated by the existence of microfluidic transistors, capacitors, and resistances, this design includes an astable multivibrator connected to N resistor-capacitor (RC) circuits as shown in Fig. 1. To create a phase delay between each RC circuit, the network has a chain topology in which each node is connected to its two nearest neighbors, with the exception of the first element, which is connected to the multivibrator and one neighbor, and the last element, which is connected to only one neighbor. The multivibrator is a transistor circuit whose output is a square wave that oscillates continuously between high and low values [9]. When one transistor (Q_1) is switched on, the other (Q_2) is switched off. At the same time, capacitor C_1 discharges while C_2 charges.

Let \mathcal{L}_1 be the Laplacian matrix associated with a chain topology, and v_i be the voltage associated with capacitor i . Let $\mathbf{v} = (v_1, \dots, v_N)^T$ and v_0 be the voltage at the transistor Q_2 , i.e., the output of the multivibrator. During the high (or low) output of the multivibrator, v_0 is constant, and the dynamics of this network system are

$$\dot{\mathbf{v}} = -\frac{1}{rc} \mathcal{L}_1 \mathbf{v} + \frac{1}{rc} (v_0 - v_1),$$

where \mathcal{L}_1 is the Laplacian matrix defined in (1). Using augmented state $\tilde{\mathbf{v}} = (v_0, \dots, v_N)^T$ and Laplacian $\tilde{\mathcal{L}}_1 \in \mathbb{R}^{N+1 \times N+1}$, the dynamics become

$$\dot{\tilde{\mathbf{v}}} = -\frac{1}{rc} \tilde{\mathcal{L}}_1 \tilde{\mathbf{v}}, \quad (3)$$

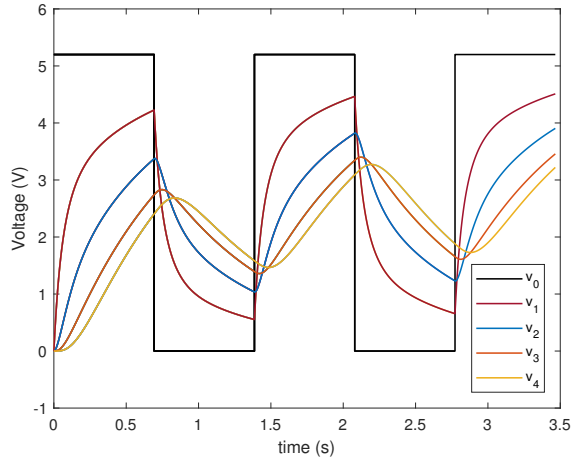


Fig. 2: Evolution of $N = 4$ RC oscillators with CPG v_0

where

$$\tilde{\mathcal{L}}_1 = \begin{bmatrix} 0 & \cdots & 0 \\ -1 & 2 & -1 & 0 & \cdots & 0 \\ 0 & -1 & 2 & -1 & 0 & \cdots & 0 \\ 0 & 0 & -1 & 2 & -1 & 0 & \cdots & 0 \\ \vdots & \vdots & \ddots & \ddots & \ddots & \ddots & \ddots & \vdots \\ \vdots & \vdots & & \ddots & \ddots & \ddots & \ddots & \ddots \\ \vdots & \vdots & & & \ddots & -1 & 2 & -1 \\ 0 & 0 & 0 & \cdots & 0 & -1 & 1 \end{bmatrix}.$$

Equation (3) essentially includes the astable multivibrator as a Central Pattern Generator that drives the network dynamics. Fig. 2 shows the results of a Matlab simulation with $v_0 = 5.2V$, $r = 1 k\Omega$, $R = 10 k\Omega$, and $C_1 = C_2 = c = 0.1 mF$. Note that, for the parameters chosen, the RC oscillators do not reach consensus, but instead show a phase lag in the rising voltage of consecutive oscillators.

We formalize this idea as follows. The period of an astable multivibrator is $\tau_0 = \ln 2(R_1 C_1 + R_2 C_2)$ and $\tau_1 = rc$ is the time constant of the RC circuit. Define the gait number

$$\eta = \frac{\tau_0}{N\tau_1} \quad (4)$$

to characterize the caterpillar-inspired gait with N legs. Let $C_1 = C_2 = c$ and $R_1 = R_2 = R$. Then, $\eta = 2 \ln(2)R/(Nr)$. Observations from simulations at various η values show that when $\eta < 1$, the contribution of the front legs to the caterpillar locomotion is negligible. On the other hand, when $\eta > 1$, all legs contribute to the locomotion. Furthermore, as η increases, the voltage outputs of legs 1 through N increases to $v_0(t)$, and the phase difference between the leg nodes decreases to 0.

B. Second-Order System: RLC Network

Next, consider a second-order model that represents each leg of the caterpillar as an RLC circuit. Although this model is currently unattainable in microfluidic circuitry, because of

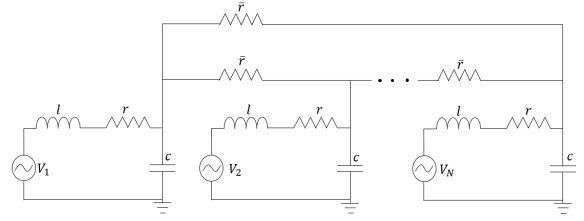


Fig. 3: Network of N RLC circuits connected through an edge resistance

the lack of microfluidic inductors, it has several attractive features for control design of networked oscillators. In particular, the RLC model illustrates how feedback at the circuit level might be used to achieve caterpillar-inspired locomotion including consensus and traveling wave solutions.

Consider an undirected graph with a circulant topology of N nodes. This graph describes the network of identical RLC oscillators coupled through an edge resistance depicted in Fig. 3. Suppose the k th RLC series circuit has resistance $r_k = r$, inductance $l_k = l$, capacitance $c_k = c$, input voltage $V_k(t)$ and edge resistance $r_{jk} = \bar{r}$. In addition, the state of oscillator k is $[v_k \ a_k]^T$, $k = 1, \dots, N$. Let $\mathbf{v} = [v_1, \dots, v_N]^T$ and $\mathbf{a} = [a_1, \dots, a_N]^T$, as before, so that the dynamics of the oscillator are

$$\frac{d}{dt} \begin{bmatrix} \mathbf{v} \\ \mathbf{a} \end{bmatrix} = M \begin{bmatrix} \mathbf{v} \\ \mathbf{a} \end{bmatrix} + \begin{bmatrix} 0 \\ \frac{1}{lc} I \end{bmatrix} V(t), \quad (5)$$

where

$$M = \begin{bmatrix} 0 & I \\ -\frac{1}{lc} I - \frac{r}{lc\bar{r}} \mathcal{L}_2 & -\frac{r}{l} I - \frac{1}{c\bar{r}} \mathcal{L}_2 \end{bmatrix},$$

$V(t) = [V_1(t), \dots, V_N(t)]^T$ is the collection of voltage inputs, one per node, and \mathcal{L}_2 is the circulant Laplacian matrix defined in (2).

Let $\mathbf{w}_r = [\mathbf{x}_r, \mathbf{y}_r]^T$ be a right eigenvector of M associated with eigenvalue λ , such that $M\mathbf{w}_r = \lambda\mathbf{w}_r$. We have

$$\mathbf{y}_r = \lambda\mathbf{x}_r$$

$$\left(\frac{-1}{lc} I - \frac{r}{lc\bar{r}} \mathcal{L}_2 \right) \mathbf{x}_r - \lambda \left(\frac{r}{l} I + \frac{1}{c\bar{r}} \mathcal{L}_2 \right) \mathbf{x}_r = \lambda^2 \mathbf{x}_r,$$

which implies

$$\mathcal{L}_2 \mathbf{x}_r = \underbrace{-c\bar{r} \frac{\lambda^2 + \frac{r}{l} + \frac{1}{lc}}{\frac{r}{l} + \lambda}}_{\triangleq \mu} \mathbf{x}_r. \quad (6)$$

Let μ be an eigenvalue of \mathcal{L}_2 associated with the vector $\chi_r = \mathbf{x}_r$. λ is a solution of

$$c\bar{r}\lambda^2 + \left(\frac{rc\bar{r}}{l} + \mu \right) \lambda + \frac{\bar{r}}{l} + \frac{r}{l}\mu = 0.$$

For the eigenvalue μ_i of \mathcal{L}_2 associated with eigenvector χ_{ri} , we can therefore define an eigenvalue of M with associated right eigenvector $\mathbf{w}_{ri} = [\chi_{ri}, \lambda_{i\pm}\chi_{ri}]^T$ as follows:

$$\lambda_{i\pm} = \frac{-\left(\frac{rc\bar{r}}{l} + \mu_i\right) \pm \sqrt{\left(\frac{rc\bar{r}}{l} + \mu_i\right)^2 - 4c\bar{r}\left(\frac{\bar{r}}{l} + \frac{r}{l}\mu_i\right)}}{2c\bar{r}}.$$

In a similar way, if we let $\mathbf{w}_z = [\mathbf{x}_z, \mathbf{y}_z]^T$ be the left eigenvectors of M associated with the eigenvalue λ such that $\mathbf{w}_z^T M = \lambda \mathbf{w}_z^T$, we have

$$\mathbf{y}_z^T \left(\frac{-1}{lc} I - \frac{r}{lc\bar{r}} \mathcal{L}_2 \right) = \lambda \mathbf{x}_z^T$$

$$\mathbf{x}_z^T - \mathbf{y}_z^T \left(\frac{r}{l} I + \frac{1}{c\bar{r}} \mathcal{L}_2 \right) = \lambda \mathbf{y}_z^T,$$

which implies

$$\mathbf{y}_z^T \mathcal{L}_2 = c\bar{r} \frac{\lambda^2 + \lambda \frac{r}{l} + \frac{1}{lc}}{\frac{r}{l} + \lambda} \mathbf{y}_z^T, \quad (7)$$

Note that (7) is similar to (6). Let $\chi_z = \mathbf{y}_z$ be the left eigenvector of \mathcal{L}_2 associated with eigenvalue μ . Thus, the corresponding left eigenvector of M is $\mathbf{w}_{zi} = [1/\lambda(-1/(lc)I - r/(lc\bar{r})\mathcal{L}_2)\chi_{zi} \quad \chi_{zi}]^T$. We have the following result.

Lemma 1: $\lambda_{i\pm}$ has negative real part, which implies the origin of the open-loop system (5) is exponentially stable.

Proof: Let $\Delta = (\frac{rc\bar{r}}{l} + \mu_i)^2 - 4c\bar{r}(\frac{\bar{r}}{l} + \frac{r}{l}\mu_i)$.

case: $\Delta > 0$

$$\mu_{max} < \frac{rc\bar{r}}{l} - 2\bar{r}\sqrt{\frac{c}{l}}$$

$$\mu_{min} > \frac{rc\bar{r}}{l} + 2\bar{r}\sqrt{\frac{c}{l}}$$

Using the results of Section II-A, we conclude that this case is impossible, since $\frac{rc\bar{r}}{l} < 2\bar{r}\sqrt{\frac{c}{l}}$ and the eigenvalues of the Laplacian are positive ($\mu > 0$).

case: $\Delta < 0$

$$\mu_{max} < \frac{rc\bar{r}}{l} + 2\bar{r}\sqrt{\frac{c}{l}}$$

$$\mu_{min} > \frac{rc\bar{r}}{l} - 2\bar{r}\sqrt{\frac{c}{l}}$$

The condition on μ_{min} is always satisfied since $\mu_{min} > 0$. In addition, $\text{Re}(\lambda_{i\pm}) < 0$, and hence $\lambda_{i\pm}$ is complex and negative.

Lemma 1 shows the origin of the open-loop system (5) is stable and the oscillations decay over time. As such, consensus may not be achieved before the oscillations die out. However, we seek to be able to sustain a rhythmic pattern over time. In order to achieve this result, we design a voltage feedback control that effectively cancels the resistance of each RLC, so as to emulate the behavior of LC circuits.

Consider the following state-feedback control, which ensures the individual oscillators in Fig. 3 converge to a common solution over time, corresponding to the caterpillar legs oscillating in synchrony. Assume a circulant topology where every node is connected both to its predecessor and successor nodes, and the head to the tail. A feedback input to (5) of the form

$$V(t) = \frac{r}{\bar{r}} \mathcal{L}_2 \mathbf{v} + rca \quad (8)$$

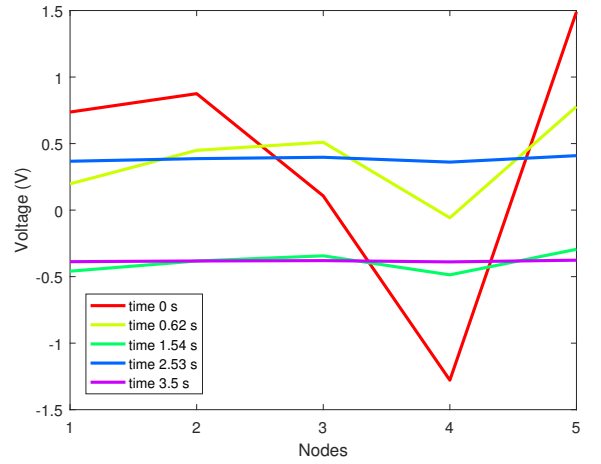
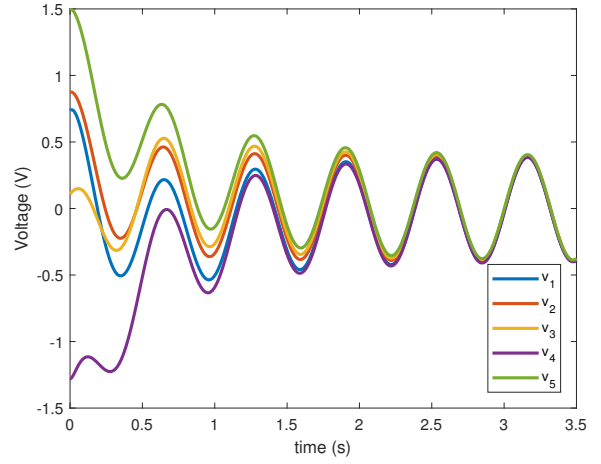


Fig. 4: $N=5$ RLC oscillators with consensus control

results in the closed-loop system

$$\frac{d}{dt} \begin{bmatrix} \mathbf{v} \\ \mathbf{a} \end{bmatrix} = \underbrace{\begin{bmatrix} 0 & I \\ -\frac{1}{lc} I & -\frac{1}{c\bar{r}} \mathcal{L}_2 \end{bmatrix}}_{\triangleq M_1} \begin{bmatrix} \mathbf{v} \\ \mathbf{a} \end{bmatrix}$$

Let $\omega_0^2 = 1/(lc)$. According to [16, Theorem 3.1], the system reaches consensus for large values of t . Specifically,

$$v_k(t) \rightarrow \frac{1}{N} [\cos(\omega_0 t) \mathbf{1}^T v(0) + \frac{1}{\omega_0} \sin(\omega_0 t) \mathbf{1}^T a(0)]$$

$$a_k(t) \rightarrow \frac{1}{N} [-\omega_0 \sin(\omega_0 t) \mathbf{1}^T v(0) + \cos(\omega_0 t) \mathbf{1}^T a(0)],$$

where $(1/N)\mathbf{1} = \mathbf{p} \in \mathbb{R}^N$ satisfies $\mathbf{p} \geq 0$, $\mathbf{p}^T \mathcal{L}_2 = 0$, and $\mathbf{p}^T \mathbf{1}_N = 1$. Each oscillator evolves at its own phase and amplitude until the network reaches a consensus (see Fig. 4). The consensus amplitude is a weighted average of the initial conditions, and the phase is arbitrary. Matlab simulations were computed using $r = 0.5 \Omega$, $c = 0.1 F$, $l = 0.1 H$, and $\bar{r} = 0.5 \Omega$. Note the consensus phase is determined by initial conditions.

To regulate the phase of the output voltages under the consensus control we invoke a deCentralized Pattern Generator (dCPG). The dCPG is a rhythmic pattern generator designed as a virtual LC circuit labeled $k=0$, that takes weak feedback from the network. Node $k=0$ is connected to node $k=1$. Let $r_{10} = \bar{r}$ denote the coupling strength from node 0 to node 1, whereas $r_{01} = \epsilon \bar{r}$ is the coupling strength from node 1 to node 0. The dynamics of node 0 are

$$\ddot{v}_0 + \frac{\epsilon}{lc}(v_0 - v_1) = \frac{1}{lc}V_0(t).$$

The modified network dynamics, including the dCPG node, are described using the $(N+1)$ -dimensional Laplacian matrix

$$\tilde{\mathcal{L}}_2 = \begin{bmatrix} \epsilon & -\epsilon & 0 & 0 & 0 & \cdots & 0 & 0 \\ -1 & 3 & -1 & 0 & 0 & \cdots & 0 & -1 \\ 0 & -1 & -2 & -1 & 0 & \cdots & 0 & 0 \\ \vdots & \ddots & \ddots & \ddots & \ddots & & & \vdots \\ \vdots & & \ddots & \ddots & \ddots & \ddots & & \vdots \\ \vdots & & & \ddots & \ddots & \ddots & \ddots & \vdots \\ \vdots & & & & \ddots & -1 & 2 & -1 \\ 0 & -1 & 0 & \cdots & & -1 & 2 \end{bmatrix}$$

Let $\tilde{\mathbf{v}} = [v_0, \dots, v_N]^T$, $\tilde{\mathbf{a}} = [a_0, \dots, a_N]^T$, as before, and $\tilde{\mathbf{r}} = \text{diag}(0, r, \dots, r)^T$. The dynamics of the $N+1$ network of oscillators with dCPG becomes

$$\frac{d}{dt} \begin{bmatrix} \tilde{\mathbf{v}} \\ \tilde{\mathbf{a}} \end{bmatrix} = \tilde{M} \begin{bmatrix} \tilde{\mathbf{v}} \\ \tilde{\mathbf{a}} \end{bmatrix} + \begin{bmatrix} 0 \\ \frac{1}{lc}\tilde{I} \end{bmatrix} \tilde{V}(t), \quad (9)$$

where

$$\tilde{M} = \begin{bmatrix} \tilde{0} & \tilde{I} \\ -\frac{1}{lc}\tilde{I} - \frac{\tilde{r}}{lc\bar{r}}\tilde{\mathcal{L}}_2 & -\frac{\tilde{r}}{lc}\tilde{I} - \frac{1}{c\bar{r}}\tilde{\mathcal{L}}_2 \end{bmatrix},$$

$\tilde{V}(t) = [V_0(t), \dots, V_N(t)]^T$ is the collection of voltage inputs, and $\tilde{0}$ and \tilde{I} are the corresponding zero and identity matrices.

Consider a feedback input similar to (8), i.e.,

$$\tilde{V}(t) = \frac{\tilde{r}}{lc}\tilde{\mathcal{L}}_2\tilde{\mathbf{v}} + \tilde{r}c\tilde{\mathbf{a}},$$

which results in the closed-loop system

$$\frac{d}{dt} \begin{bmatrix} \tilde{\mathbf{v}} \\ \tilde{\mathbf{a}} \end{bmatrix} = \underbrace{\begin{bmatrix} \tilde{0} & \tilde{I} \\ -\frac{1}{lc}\tilde{I} & -\frac{1}{c\bar{r}}\tilde{\mathcal{L}}_2 \end{bmatrix}}_{\triangleq M_2} \begin{bmatrix} \tilde{\mathbf{v}} \\ \tilde{\mathbf{a}} \end{bmatrix}.$$

Under the closed-loop control with dCPG, the network reaches consensus with node $k=0$. If $\epsilon > 0$, the network of oscillators influence the dCPG, whereas if $\epsilon = 0$, $(v_k(t), a_k(t))$ converge to $(v_0(t), a_0(t))$ as $t \rightarrow \infty$ (see Fig. 5), and

$$v_0(t) = \cos(\omega_0 t)v_0(0) + \frac{1}{\omega_0^2} \sin(\omega_0 t)a_0(0)$$

$$a_0(t) = -\omega_0 \sin(\omega_0 t)v_0(0) + \cos(\omega_0 t)a_0(0).$$

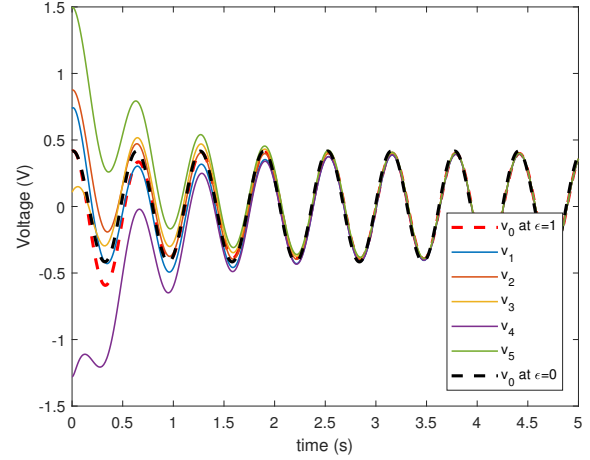


Fig. 5: Evolution of $N=5$ RLC oscillators with dCPG and consensus feedback control

Next, consider a feedback controller that achieves a stable traveling wave, i.e., the output propagates around the oscillator network like the traveling wave observed in caterpillar locomotion. The feedback input to (5)

$$V(t) = \mathbf{v} + rca + \frac{l}{\bar{r}}\mathcal{L}_2\mathbf{a},$$

yields $\dot{\mathbf{v}} = \mathbf{a}$, and $\dot{\mathbf{a}} = -r/(lc\bar{r})\mathcal{L}_2\mathbf{v}$, corresponding to the closed-loop system

$$\frac{d}{dt} \begin{bmatrix} \mathbf{v} \\ \mathbf{a} \end{bmatrix} = \underbrace{\begin{bmatrix} 0 & I \\ \frac{-r}{lc\bar{r}}\mathcal{L}_2 & 0 \end{bmatrix}}_{\triangleq M_3} \begin{bmatrix} \mathbf{v} \\ \mathbf{a} \end{bmatrix} \quad (10)$$

Because the network is undirected and circulant, the Laplacian \mathcal{L}_2 is the finite-difference approximation of a 2nd-order spatial derivative. Specifically, at node k , $\ddot{v}_k = d^2v_k/dt^2$ and $\mathcal{L}_{2,k}\mathbf{v} = -v_{k-1} + 2v_k - v_{k+1}$, where $\mathcal{L}_{2,k}$ is the k^{th} row of \mathcal{L}_2 . Let x_k denote the position of node k and $v(x, t)$ a spatially continuous representation of $\mathbf{v}(t)$, e.g., for large N . We have

$$-\mathcal{L}_{2,k}\mathbf{v} = v_{k-1} - 2v_k + v_{k+1} \approx \Delta x^2 \frac{d^2v}{dx^2} \Big|_{x=x_k}$$

where Δx is the (uniform) spacing between the legs of the caterpillar. Thus, (10) approximates the partial differential wave equation

$$\frac{\partial^2 v}{\partial t^2} = \underbrace{\frac{r}{lc\bar{r}}\Delta x^2}_{\triangleq \gamma} \frac{\partial^2 v}{\partial x^2},$$

which has solution $v(x, t) = 1/2 [f(x + \gamma t) + f(x - \gamma t)]$ for $v(x, 0) = f(x)$ [23]. Choosing $a(x, 0) = (\gamma/2)(df/dx)$ yields a one-directional wave, as shown in Fig. 6.

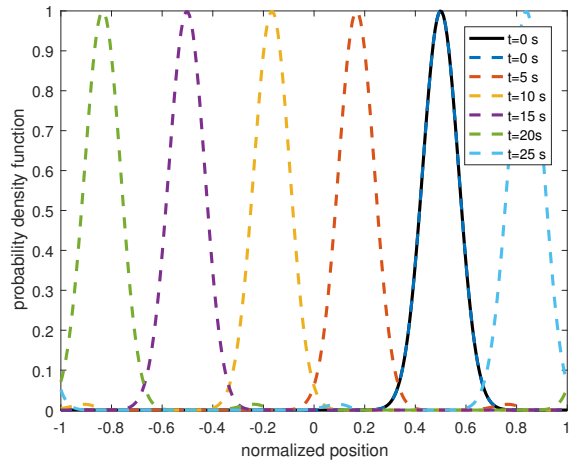


Fig. 6: Propagation of wave in time

IV. EXPERIMENTAL RESULTS

We fabricated an astable multivibrator (see Fig. 1) using 3D-printed microfluidic transistors and microfluidic capacitors [21]. For the resistors, we used various lengths of the connector (Tygon microbore tubing, 06420-03, Cole Parmer, Vernon Hills, IL). The internal resistors were three times larger than the external ones, which gave the capacitors the opportunity to fully charge before switching. We used the MAESFLO system (Fluigent, Paris, France), which includes a Microfluidic Flow Control System and a FLOWELL microfluidic flow sensor, and the Sensirion SLI-1000 flow sensor to regulate the input pressures while simultaneously monitoring the flow rates through the 3D-printed devices. We used Tygon microbore tubing and micro pipe fittings to connect the circuit components. We conducted all experiments at room temperature environment (20–25° C).

To examine the performance of the circuit, we connected the input point to the Fluigent system and the output to the flow unit. Using the Fluigent MAESFLO software, we incrementally increased the pressure within the circuit. Once all the air bubbles were out of the circuit and the pressure stabilized at a constant value (usually around 200–250 mbar), we collected data from the flow unit, plotted in Fig. 7. These preliminary results indicate the output pressure oscillates as expected. Moreover, the results correlates that of an electronic astable multivibrator with capacitance $C_1 = C_2 = 0.1$ mF, resistance $R_1 = R_2 = 10$ k Ω , and a period $\tau_0 \approx 0.6932$ seconds.

V. CONCLUSION

Caterpillar locomotion enables robust, albeit slow, navigation of irregular terrains. It is initiated from the tail to the front, and each left-right pair of legs is lifted simultaneously. We used RC and RLC oscillators to mimic the locomotory pattern of the caterpillars as a precursor to a microfluidic fabrication design. We characterized the locomotion gait in the RC network, and designed a closed-loop control for

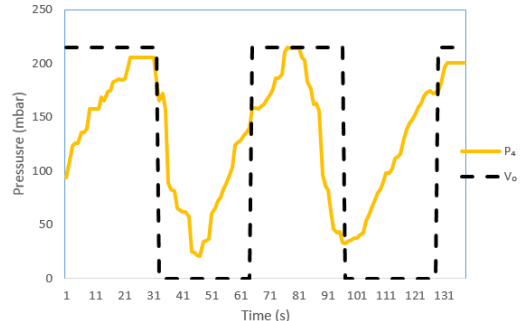
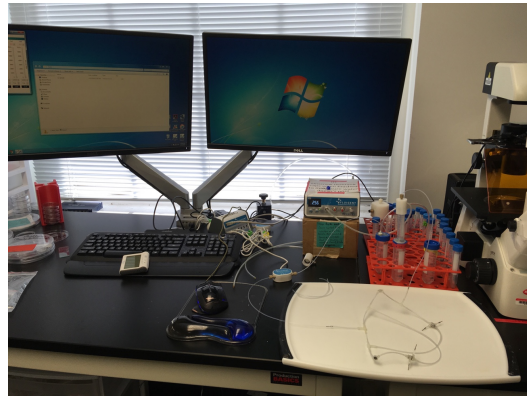


Fig. 7: Experimental set-up and multivibrator output pressure from experiment with constant input pressure 230 mbar.

consensus and traveling wave solution in the RLC network. A dCPG was successfully implemented as an input to the RLC network to regulate the collective phase. Preliminary experimental results for the microfluidic testbed are included. In ongoing work, we seek to implement the RC circuit design in microfluidics and design fluidic leg actuators for a soft-robotic caterpillar.

VI. ACKNOWLEDGEMENTS

We acknowledge support of Joshua Hubbard and Ryan Sochol for the microfluidic experiments.

REFERENCES

- [1] M. Wehner, R. L. Truby, D. J. Fitzgerald, B. Mosadegh, G. M. Whitesides, J. A. Lewis, and R. J. Wood, “An integrated design and fabrication strategy for entirely soft, autonomous robots,” *Nature*, vol. 536, no. 7617, pp. 451–455, 2016.
- [2] F. Saunders, E. Golden, R. D. White, and J. Rife, “Experimental verification of soft-robot gaits evolved using a lumped dynamic model,” *Robotica*, vol. 29, no. 6, pp. 823–830, 2011.
- [3] R. F. Shepherd, F. Ilievski, W. Choi, S. A. Morin, A. A. Stokes, A. D. Mazzeo, X. Chen, M. Wang, and G. M. Whitesides, “Multigait soft robot,” *Proceedings of the National Academy of Sciences*, vol. 108, no. 51, pp. 20400–20403, 2011.
- [4] D. W. Schuldt, J. Rife, and B. Trimmer, “Template for robust soft-body crawling with reflex-triggered gripping,” *Bioinspiration & biomimetics*, vol. 10, no. 1, p. 016018, 2015.
- [5] B. A. Trimmer, A. E. Takesian, B. M. Sweet, C. B. Rogers, D. C. Hake, and D. J. Rogers, “Caterpillar locomotion: A new model for soft-bodied climbing and burrowing robots,” in *7th International Symposium on Technology and the Mine Problem*, vol. 1, pp. 1–10, Monterey, CA: Mine Warfare Association, 2006.
- [6] L. van Griethuijsen and B. Trimmer, “Locomotion in caterpillars,” *Biological Reviews*, vol. 89, no. 3, pp. 656–670, 2014.

- [7] S. Vedel, *Millisecond dynamics in microfluidics: Equivalent circuit theory and experiment*. PhD thesis, DTU Nanotech, Department of Micro and Nanotechnology, 2009.
- [8] R. D. Sochol, E. Sweet, C. C. Glick, S. Venkatesh, A. Avetisyan, K. F. Ekman, A. Raulinaitis, A. Tsai, A. Wienkers, K. Korner, K. Hanson, A. Long, B. J. Hightower, G. Slatton, D. C. Burnett, T. L. Massey, K. Iwai, L. P. Lee, K. S. J. Pister, and L. Lin, "3D printed microfluidic circuitry via multijet-based additive manufacturing," *Lab on a Chip*, vol. 16, pp. 668–678, 2016.
- [9] A. S. Sedra and K. C. Smith, *Microelectronic circuits theory and applications*. Oxford University Press.
- [10] F. Saunders, B. A. Trimmer, and J. Rife, "Modeling locomotion of a soft-bodied arthropod using inverse dynamics," *Bioinspiration & biomimetics*, vol. 6, no. 1, p. 016001, 2010.
- [11] T. Umedachi and B. A. Trimmer, "Autonomous decentralized control for soft-bodied caterpillar-like modular robot exploiting large and continuum deformation," in *Intelligent Robots and Systems (IROS), 2016 IEEE/RSJ International Conference on*, pp. 292–297, IEEE, 2016.
- [12] T. Umedachi, K. Takeda, T. Nakagaki, R. Kobayashi, and A. Ishiguro, "Fully decentralized control of a soft-bodied robot inspired by true slime mold," *Biological cybernetics*, vol. 102, no. 3, pp. 261–269, 2010.
- [13] T. Vicsek and A. Zafeiris, "Collective motion," *Physics Reports*, vol. 517, no. 3, pp. 71–140, 2012.
- [14] D. A. Paley, N. E. Leonard, R. Sepulchre, D. Grunbaum, and J. K. Parrish, "Oscillator models and collective motion," *IEEE Control Systems*, vol. 27, no. 4, pp. 89–105, 2007.
- [15] R. C. Dorf and J. A. Svoboda, *Introduction to electric circuits*. John Wiley & Sons, 2010.
- [16] W. Ren, "Synchronization of coupled harmonic oscillators with local interaction," *Automatica*, vol. 44, no. 12, pp. 3195–3200, 2008.
- [17] W. Ren and R. W. Beard, *Distributed consensus in multi-vehicle cooperative control*. Springer, 2008.
- [18] R. Sepulchre, D. A. Paley, and N. E. Leonard, "Stabilization of planar collective motion: All-to-all communication," *IEEE Transactions on Automatic Control*, vol. 52, no. 5, pp. 811–824, 2007.
- [19] W. Ren, R. W. Beard, and T. W. McLain, "Coordination variables and consensus building in multiple vehicle systems," in *Cooperative Control*, pp. 171–188, Springer, 2005.
- [20] R. W. Beard and V. Stepanyan, "Information consensus in distributed multiple vehicle coordinated control," in *42nd IEEE Conference on Decision and Control*, vol. 2, pp. 2029–2034, IEEE, 2003.
- [21] R. D. Sochol, E. Sweet, C. C. Glick, S. Venkatesh, A. Avetisyan, K. F. Ekman, A. Raulinaitis, A. Tsai, A. Wienkers, K. Korner, K. Hanson, A. Long, B. J. Hightower, G. Slatton, D. C. Burnett, T. L. Massey, K. Iwai, L. P. Lee, K. S. J. Pister, and L. Lin, "3D printed microfluidic circuitry via multijet-based additive manufacturing," *Lab on a Chip*, vol. 16, no. 4, pp. 668–678, 2016.
- [22] K. W. Oh, K. Lee, B. Ahn, and E. P. Furlani, "Design of pressure-driven microfluidic networks using electric circuit analogy," *Lab on a Chip*, vol. 12, no. 3, pp. 515–545, 2012.
- [23] S. J. Farlow, *Partial differential equations for scientists and engineers*. Courier Corporation, 1993.